

Supporting Information

Janus Membrane with Novel Directional Water Transport Capacity for Efficient Atmospheric Water Capture

*Baona Ren, Haohong Pi, Xin Zhao, Miaomiao Hu, Xiuqin Zhang, Rui Wang, Jing Wu**

Beijing Key Laboratory of Clothing Materials R & D and Assessment, Beijing Engineering Research Center of Textile Nanofiber, School of Materials Design & Engineering, Beijing Institute of Fashion Technology, Beijing 100029, China
E-mail: a.wujing@163.com_(J. Wu)

S1: XRD and FTIR spectrum of as-prepared samples

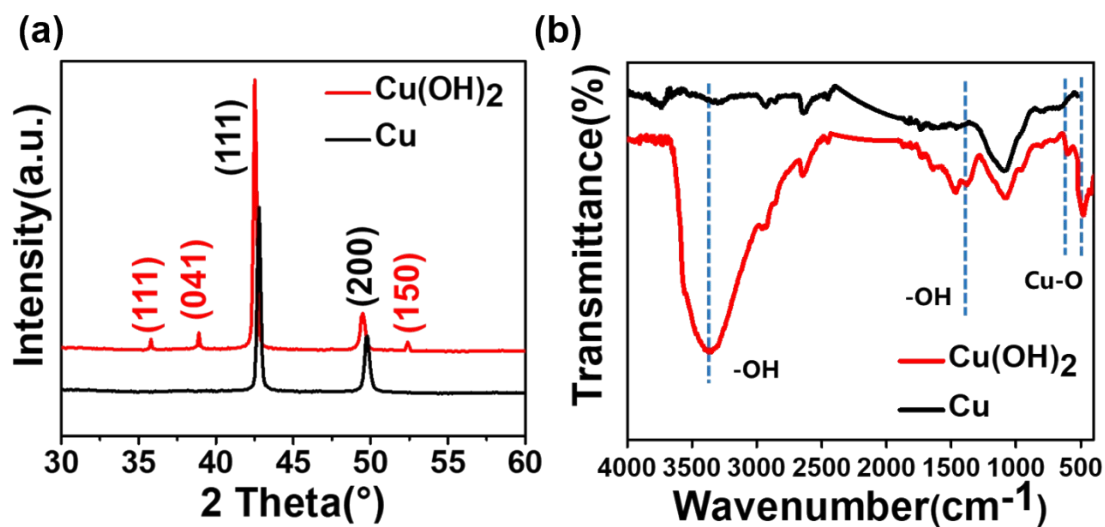


Fig. S1 (a) XRD pattern of the pristine Cu mesh wire and Cu(OH)₂ mesh wire. (b) FTIR spectrum of the pristine Cu mesh wire and Cu(OH)₂ mesh wire.

The X-ray diffraction (XRD) pattern demonstrated that the nanosheets were orthorhombic-phase Cu(OH)₂ crystals, which was in accordance with the values in the standard card (JCPDS Card No. 13-420) (Fig. S1(a)). Whereas the extremely strong (111) and (200) peaks corresponded to the pristine Cu mesh.¹ To further verify the formation of Cu(OH)₂ during the oxidation process, FTIR analysis was carried out. As shown in Fig. S1(b), compared with the pristine Cu mesh, several new peaks appeared in the spectrum after oxidation. The peaks at 3371 and 1464 cm⁻¹ were assigned to the stretching and bending modes of the hydroxyl groups in Cu(OH)₂. The Cu-O-H bending vibrations were observed at 604 and 500 cm⁻¹.^{2,3} These results indicated that Cu(OH)₂ was formed during the oxidation process.

S2: SEM images and statistics analysis of fiber diameter

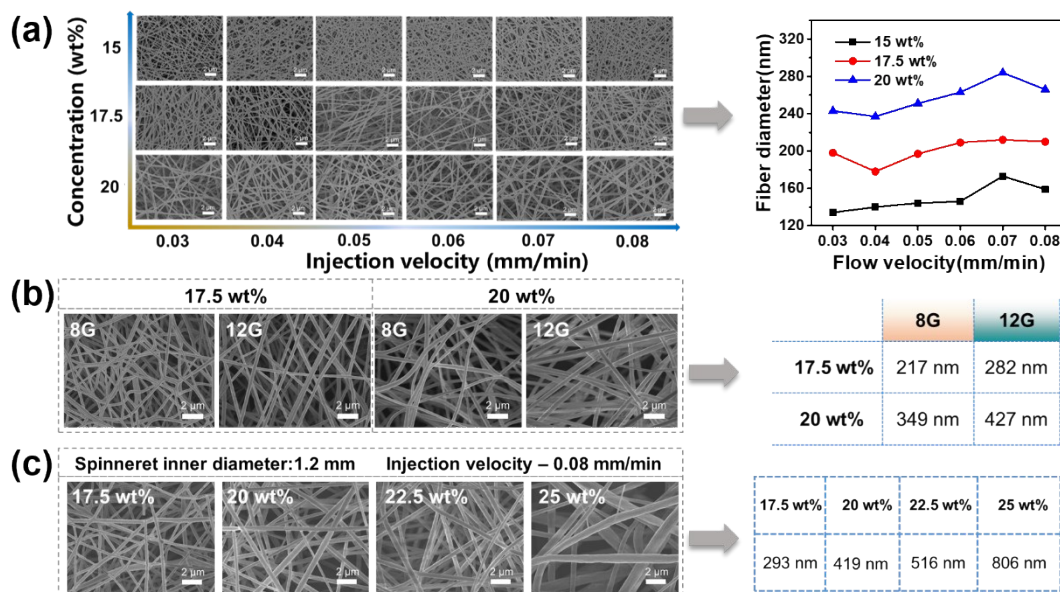


Fig. S2 Morphologies and average fiber diameters of the as-prepared electrospun PVDF-HFP/F fibrous membranes. (a) The PVDF-HFP/F fibers prepared with different electrospun solution concentration of 15, 17.5, 20 wt% and injection velocity of 0.03, 0.04, 0.05, 0.06, 0.07, 0.08 (the spinneret inner diameter was 0.6 mm). (b) The PVDF-HFP/F-17.5 wt%-8G, -12G, PVDF-HFP/F-20 wt%-8G, and-12G electrospun fibers. (c) The PVDF-HFP/F nanofiber membranes obtained at various concentration of 17.5 wt%, 20 wt%, 22.5 wt% and 25 wt%. (8G:0.8 mm, 12G:1.2 mm)

To explore the effect of the electrospun solution concentration, injection velocity and the spinneret inner diameter to membrane morphology, a series of experiments were designed in this work. The corresponding SEM images of PVDF-HFP/F fibrous membrane are shown in Fig. S2. Firstly, the effect of electrospun solution concentration and injection velocity was studied. The fibers were prepared at solution concentrations of 15, 17.5 and 20 wt%, with injection velocities ranging from 0.01 to 0.08 mm/min (the spinneret inner diameter was 0.6 mm). The result showed that the fiber morphology changed more obviously with the electrospun solution concentration (Fig. S2(a)). Then, the effect of the spinneret inner diameter was studied. As can be seen from Fig. S2(b),

the spinneret diameter had little effect on fiber morphology. Therefore, the PVDF-HFP/F fibrous membranes prepared at different electrospun concentrations were further studied (Fig. S2(c)). It can be found that the electrospun solution concentration plays major influence on membrane morphology in this work.

S3: EDS mappings of the cross-section of hybrid Janus membrane

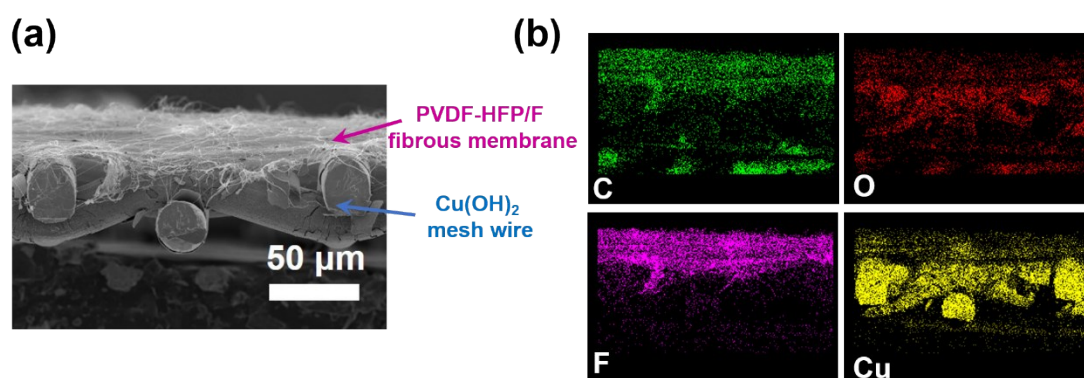


Fig. S3 (a) Original SEM image of the hybrid Janus membrane. (b) EDS mappings of the cross-section of the hybrid Janus membrane.

Table S1(a) EDS results of the cross-section of the hybrid Janus membrane

	Elements	C	O	F	Cu
Hybrid Janus membrane	PVDF-HFP/F fibrous membrane	✓	✓	✓	✗
	Cu(OH) ₂ mesh wire	✓	✓	✗	✓

Table S1(b) Element contents of the cross-section of the hybrid Janus membrane

Element contents (wt%)	C	O	F	Cu
Hybrid Janus membrane	27.42	11.64	22.88	38.05

Fig. S3(a) and Fig. S3(b) are the SEM image of the cross-section of the hybrid Janus membrane and its EDS mappings regarding to the contained elements. It can be seen that the hybrid Janus membrane composed by two layers, one thinner layer was PVDF-HFP/F fibrous membrane, and the other layer with thicker wire was Cu(OH)₂ mesh wire. EDS mappings are further confirmed that both the PVDF-HFP/F and Cu(OH)₂ layers contained C (marked in green color) and O (marked in red color) elements. The element F (marked in rose red color) only existed in PVDF-HFP/F fibrous layer, and Cu (marked in yellow) only existed in Cu(OH)₂ layer. The details of element contents are listed in Table S1(b).

S4: Detailed schematic illustration of the adhesion force testing process

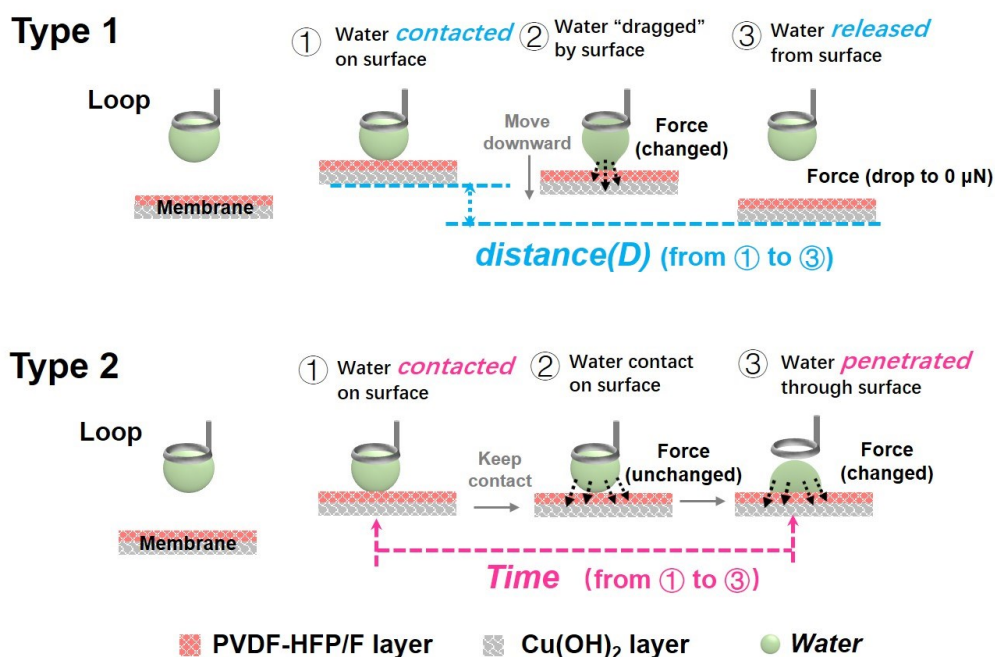


Fig. S4 Detailed experimental process of adhesive force measure.

Herein, two types of methods have been provided to measure the adhesive force between water droplet and the membrane surface.

Type 1: Water droplet was suspended and fixed on a metal loop. ①Firstly, water droplet contacted on the membrane surface. ②Then the surface moved downward immediately. At this time, water droplet was dragged by the force provided by the surface. As the surface continuing moving downward, the water droplet was stretched. ③Once water droplet was separated or pulled off from the surface, the surface stop moving. The distance from state ① to state ③ and the force change during the process have been recorded. Thus, the Distance(D)-Adhesive force curve can be obtained.

Type 2: Water droplet was still suspended and fixed on the metal loop. ①Water droplet contacted on the surface. ②Water droplet keep contacting on the surface rather than surface or water droplet moving. ③For a period of time, once water droplet penetrated

though the membrane, the adhesive force changed. When the water droplet was fully penetrated, the force finally dropped to zero. During this process, the time from state ① to state③ and the force change have been recorded. Accordingly, the Time-Adhesive force curve can be obtained.

S5: The relationships of the electrospinning time, membrane thicknesses and unidirectional water transport

Table S2 Relationships of membrane the electrospinning time, membrane thicknesses and unidirectional water transport

Electrospinning time (s)	PVDF-HFP/F-810/Cu(OH) ₂	Unidirectional water transport		PVDF-HFP/F-290/Cu(OH) ₂	Unidirectional water transport	
	Thickness (μm)	Transport ↕Yes	No transport ↕No	Thickness (μm)	Transport ↕Yes	No transport ↕No
10	124.87 ± 0.24		↕No	124.48 ± 0.15		↕No
20	125.03 ± 0.15	↕Yes		124.65 ± 0.23		↕No
30	125.23 ± 0.17	↕Yes		124.65 ± 0.25	↕Yes	
40	125.42 ± 0.21	↕Yes		124.83 ± 0.32	↕Yes	
60	125.78 ± 0.13	↕Yes		125.33 ± 0.41	↕Yes	
90	125.82 ± 0.41	↕Yes		125.75 ± 0.35	↕Yes	
120	126.52 ± 0.21		↕No	125.92 ± 0.17		↕No
150	126.75 ± 0.20		↕No	1126.15 ± 0.35		↕No
180	127.08 ± 0.14		↕No	126.70 ± 0.28		↕No

In this work, the thickness and water transport capacity of the hybrid Janus membrane were adjusted by regulating the electrospinning time of the PVDF-HFP/F fibrous membrane. The electrospinning time ranged from 0 to 180 s. Table S2 exhibited the detailed relationships of the electrospinning time, membrane thicknesses and unidirectional water transport capacity.

S6: Water trapping system for atmospheric water capture measurement

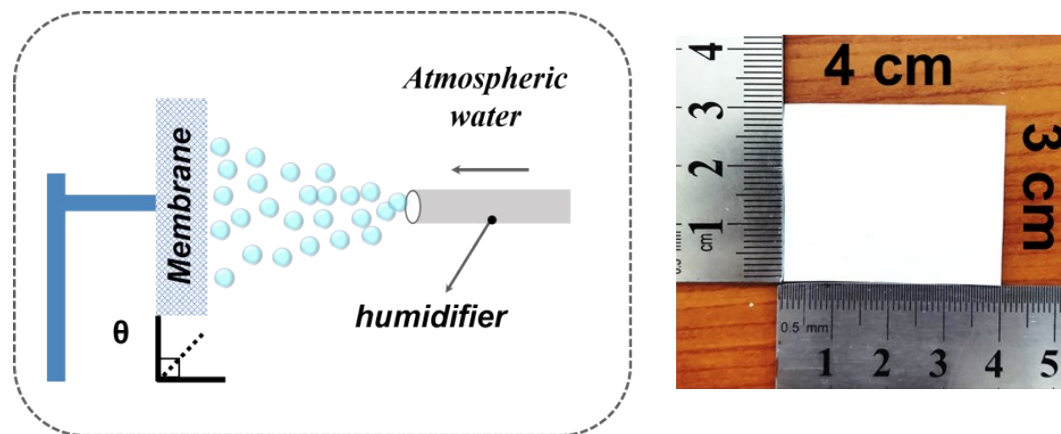


Fig. S6 Water trapping system (left) and sample size (right)

S7: The moisture trapping capacities of hybrid Janus membrane with different pore size under various water droplets velocity

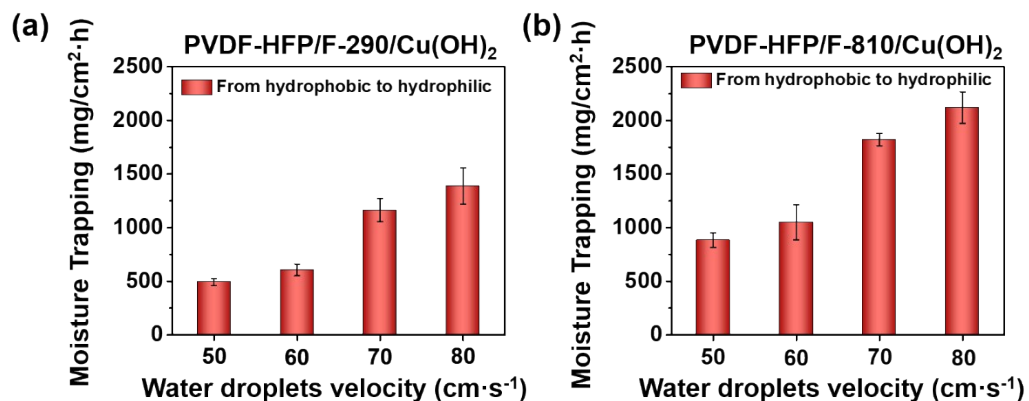


Fig. S7 Moisture trapping amount of (a) PVDF-HFP/F-290/Cu(OH)₂ and (b) PVDF-HFP/F-810/Cu(OH)₂ under the water droplets velocity of 50, 60, 70 and 80 cm·s⁻¹.

According to Fig. S7(a) and S7(b), it can be seen that the pore size of the membrane plays roles in the moisture trapping capacity. The PVDF-HFP/F-810/Cu(OH)₂ (pore size~1.78±0.69 μm) exhibited higher moisture trapping amount than that of PVDF-HFP/F-290/Cu(OH)₂ (pore size~633±19 nm). Meanwhile, the water droplets velocity also has effect on moisture trapping capacity, i.e., the moisture trapping amount increased with the increasing of water droplets velocity.

S8: Comparison of moisture trapping capacity of Janus membranes at different tilt angles.

Table S3 Moisture trapping capacities of the Janus PVDF-HFP/F-810/Cu(OH)₂ and PVDF-HFP/F-810/Cu(OH)₂ membranes at different tilt angles.

The tilt angle	Moisture trapping capacity (mg·cm ⁻² ·h ⁻¹)			
	PVDF-HFP/F-810/Cu(OH) ₂		PVDF-HFP/F-290/Cu(OH) ₂	
	Hydrophobic to hydrophilic	Hydrophilic to hydrophobic	Hydrophobic to hydrophilic	Hydrophilic to hydrophobic
0°	58.5 ± 17.39	37.67 ± 8.80	68.80 ± 16.45	37.00 ± 10.93
45°	1150 ± 168.30	477.3 ± 56.55	764.10 ± 109.31	189.60 ± 29.13
90°	1821 ± 56.18	676.53 ± 68.75	1162 ± 109.06	249.40 ± 62.94

References

- 1 L. L. Hou, N. Wang, X. K. Man, Z. M. Cui, J. Wu, J. C. Liu, S. Li, Y. Gao, D. M. Li, L. Jiang and Y. Zhao, *ACS Nano*, 2019, **13**, 4124-4132.
- 2 C. F. Li, Y. D. Yin, H. G. Hou, N. Y. Fan, F. L. Yuan, Y. M. Shi and Q. L. Meng, *Solid State Commun.*, 2010, **150**, 585-589.
- 3 A. Pramanik, S. Maiti and S. Mahanty, *Dalton Trans.*, 2015, **44**, 14604-14612.